Thin hydrogel coatings formation catalyzed by immobilized enzyme horseradish peroxidase

Christian Wischke[1], Marlin Kersting[1,2], Alexander Welle[2], Liudmila Lysyakova[1], Steffen Braune[1], Karl Kratz[1], Friedrich Jung[1], Matthias Franzreb[2], Andreas Lendlein[1,3]

[1]Institute of Biomaterial Science and Berlin-Brandenburg Center for Regenerative Therapies, Helmholtz-Zentrum Geesthacht, Kantstr. 55, 14513 Teltow, Germany
[2]Institute of Functional Interfaces, Karlsruhe Institute of Technology, Hermann-von-Helmholtz-Platz 1, 76344 Eggenstein-Leopoldshafen, Germany
[3]Institute of Chemistry, University of Potsdam, Karl-Liebknecht-Str. 24-25, 14476 Potsdam, Germany
*Correspondence: christian.wischke@hzg.de

ABSTRACT

Enzymes can be a renewable source of catalytic agents and thus be interesting for sustainable approaches to create and modify functional materials. Here, thin hydrogel layers were prepared as thin coatings on hard substrates by immobilized horseradish peroxidase. Hydrophilic 4-arm star shaped telechelics from oligo(ethylene glycol) bearing on average 55% end groups derived from aromatic amino acids served as monomers and enzymatic substrates. Shifts of the contact angle from 84° to 62° for the wetting process and of zeta potential towards the neutral range illustrated an alteration of physicochemical properties of the model surfaces by a hydrophilic shielding. Time-of-flight secondary ion mass spectrometry (ToF-SIMS), quartz crystal microbalance and atomic force microscopy (AFM) experiments enabled the qualitative and quantitative proof of hydrogel deposition at the interface with thicknesses in the medium nanometer size range. Conceptually, as the immobilized enzyme becomes entrapped in the hydrogel and the crosslinking mechanism bases on a radical reaction after enzymatic activation of the monomers with a limited diffusivity and lifetime, the formed network material can be assumed to be inhomogeneous on the molecular level. On the macroscale, however, relative homogeneity of the coating was observed via ToF-SIMS and AFM mapping. As an exemplary functional evaluation in view of bioanalytical applications, the thrombogenicity of the coating was studied in static tests with human blood from several donors. In the future, this "coating-from" approach may be explored for cell culture substrate coatings, for protein/biofilm repellence in technical applications, or in bioanalytical devices.

INTRODUCTION

Technologies for modification of material surfaces to create envisioned interfacial properties are of great technological interest, particularly when it comes to *in situ* thin layer coatings with very hydrophilic materials, i.e. hydrogels, on hard hydrophobic materials.

While spin-coating of precursors onto the surface and crosslinking of reactive moieties via UV irradiation or ionic crosslinking has been successfully applied to flat materials [1] [2], and approaches that conceptually could be used at any surface shape are also of interest. For matrix materials that are themselves swellable, the deposition of molecules dissolved in the swelling agent at the material surface during solvent uptake has been reported, i.e., the swellable matrix filters out precursor materials that gel at its surface [3]. For non-swelling materials of any shape, chemical grafting approaches may be used, where either preformed oligomers are coupled to the surface or catalysts are bound to allow synthesis of shielding layers at the surface from dissolved monomers [4]. Furthermore, inspired by muscle adhesion strategies through catecholic amino acids, the spontaneous multistep reaction of dopamine under weakly alkaline conditions to polydopamine can be applied to modify various types of material surfaces [5]. Typically, low thicknesses of the coating close to the diameter of the respective polymer coil may be expected by these approaches. To obtain a slightly thicker coating, multiple layers e.g. of oppositely charged polymers may be deposited or polymer networks may be synthesized [6].

In this context, green chemistry approaches for polymer network synthesis at interfaces avoiding hazardous solvents and relying on renewable sources of catalytic agents can contribute to sustainable technologies. Here, enzymes are of interest, which already are of extensive importance in cell-free biotechnology [7], which may also be reusable when bound to solid support materials. Accordingly, a substantial body of literature reports on enzyme immobilization strategies as basis for various applications [8]. Here, the capability of enzymes to crosslink polymeric precursors to form hydrogels [9] [10] may be facilitated to realize a "coating-from" rather than a "coating-to" approach for functional interfaces. Hydrophilic molecules, if equipped with motifs such as the amino acid tyrosine and its derivatives forming substrates for enzymatic conversion may be used as precursor molecules for enzyme-catalyzed hydrogel coatings. In this concept, the enzyme will residue at the surface and catalyze hydrogel formation in its environment until being fully entrapped in a hydrogel layer. Based on previous experience of relatively slow conversion of small molecule substrates by a candidate enzyme (mushroom tyrosinase) after its surface immobilization [11], alternative enzymes which react faster may be preferred for surface coating within a reasonable time frame.

Here, horseradish peroxidase (HRP), an oxidase suitable for catalyzing the crosslinking of phenolic moieties in the presence of hydrogen peroxide [12] [13] [14], should be evaluated for surface-bound formation of thin hydrogel layers. Star-shaped oligo(ethylene glycol) (sOEG) bearing on average 55% desamino tyrosine (DAT) moieties were employed as a substrate and hydrogel precursor. A particular focus was to demonstrate the successful synthesis and deposition of thin layer hydrogel on glass as a model for a hard material and illustrate the function of this coating in a demonstration experiment.

EXPERIMENTAL

Sample preparation methods

For HRP immobilization on glass surfaces, amino functionalized glass (Nexerion Slide A+, Schott, Germany) was cut to size of e.g. 25 × 15 mm^2, rinsed with ultrapure water, incubated in 2.5 vol.% glutaraldehyde solution pH 5.2 (Sigma Aldrich, Germany) at room temperature under agitation at 120 rpm for 1 h, washed four times for 2 min with ultrapure water and incubated with 0.5 mg·ml^{-1} HRP (Type VI, ≥ 250 U·mg^{-1}; Sigma-Aldrich, Germany) solution in 0.1 M sodium phosphate buffer of either pH 6 or pH 7.1 under agitation at 120 rpm for 2 h. Subsequently, non-bound HRP was removed by washing twice with 0.1 M TRIS containing 1 M NaCl (pH 9) followed by washing three-times with 0.1 M TRIS (pH 9).

Gold surfaces were functionalized with HRP in the context of Quartz Crystal Microbalance (QCM) experiments, where the QCM sensors with a gold top layer were first cleaned by plasma treatment (20 min, UV/Ozone ProCleaner Plus, Bioforce Nanosciences, USA) and then immediately incubated in 1 mM ethanolic solution of 11-amino-1-undecanethiol hydrochloride for 24 h to introduce amino groups in a self-assembled monolayer (for further steps, see characterization section).

Thin layer hydrogel coatings were prepared from precursors (for synthesis and characterization see [15]) composed of 4 arm sOEG (10 kDa, JenKem Technology, Japan; MALDI-MS: M_n 10.3 kDa) functionalized with DAT. The degree of DAT functionalization *d.f.* was 55% as determined by NMR in DMSO-d$_6$ by relating the aromatic protons of DAT (δ=6.6 ppm; CH$_2$CC*H*) to the signals of sOEG repetitive units (δ=3.5 ppm; OC*H*$_2$). Considering the difference in contributing protons and corresponding signal intensity, the methodological error of *d.f.* determination can be estimated to be relatively high (5%), while the variation of *d.f.* in repetitive synthesis was reported to be up to 10% [15]. HRP functionalized matrix materials were incubated for 2 hours (room temp.; 95 rpm agitation) in 6.7 wt.% sOEG-DAT solution in 10 mM sodium phosphate buffer (pH 7.4) supplemented with 0.33 vol.% H$_2$O$_2$, followed by washing four times with ultrapure water.

Characterization techniques

Contact angles of surfaces at different steps in functionalization were determined in ultrapure water (55 µS·cm^{-1}) by the captive bubble method at 23 °C using a DSA 100 instrument (Krüss, Germany).

The zeta potential of the surfaces were characterized with a DelsaNano C (Beckman Coulter, Germany) using the flat surface in water (50 to 200 µS·cm^{-1}).

QCM experiments were conducted at a Q-Sense E4 QCM-D with QFM 401 flow modules (LOT-QD, Germany), with data analysis of the 5th, 7th and 9th overtone by the QTools 4.0.1 software with the Kevin-Voigt model. Using flow rates of 50 µl·min^{-1}, the system was first equilibrated by rinsing with sodium phosphate buffer (0.1 M; pH 7.1). In control experiments with HRP adsorption only, the same buffer was used for all steps and gold sensors were subsequently exposed to HRP solutions (0.5 mg·ml^{-1}), rinsed, treated with precursor solution (6.7 wt.%; containing 0.33 vol.% H$_2$O$_2$), and again rinsed, each conducted until signal equilibration. For covalent binding of HRP to amine functionalized gold sensors, the applied steps were treated with to 2.5 vol.% glutaraldehyde, rinsed, 0.5 mg·ml^{-1} HRP, rinsed, precursor solution (6.7 wt.%; containing 0.33 vol.% H$_2$O$_2$), and rinsed.

All steps employed 0.1 M sodium phosphate buffer pH 7.1, except the rinsing step after HRP functionalization, where 0.1 M TRIS pH 9 was used.

ToF-SIMS (Time-of-Flight Secondary Ion Mass Spectrometry) was performed on a TOF.SIMS5 instrument (ION-TOF GmbH, Münster, Germany), equipped with a Bi cluster primary ion source and a reflectron type time-of-flight analyzer. The ultra-high vacuum base pressure was $< 5 \times 10^{-9}$ mbar. The source was operated in the "high current bunched" mode providing short Bi_3^+ primary ion pulses at 25 keV energy and a lateral resolution of approx. 4 µm. The short pulse length of 0.8 ns allowed for high mass resolution. Primary ion doses were kept below 10^{11} ions/cm^2 (static SIMS limit). Spectra were calibrated on the omnipresent C^-, C_2^-, C_3^-, or on the C^+, CH^+, CH_2^+, and CH_3^+ peaks. Based on these datasets the chemical assignments for characteristic fragments were determined. Images larger than the maximum deflection range of the primary ion gun of 500×500 µm^2 were obtained using the manipulator stage scan mode.

Atomic force microscopy (AFM) was performed with the atomic force microscope MFP-3D-BIO (Asylum Research, Germany) in combination with the inverted optical microscope Zeiss Axio Observer Z1 (Carl Zeiss AG, Germany) in Millipore-water at room temperature in AC mode. Soft gold-coated Silicon Nitride cantilevers with spring constants k=0.02 N/m (iDrive long tip, Asylum Research, Germany) and k=0.03 N/m (MLCT-D, Bruker, Germany) were used. Via scratching the surface prior to analysis, coating thickness was estimated from the Z-sensor data.

Platelet adhesion and activation after sample exposure for 60 min were characterized in a quasi-static test. The study was carried out according to a previously published consensus protocol using adjusted fresh platelet rich plasma from characterized healthy humans (n=3 donors) [16]. The study received an approval of the responsible ethics committee (# EA2-018-16; Charité University Medicine Berlin, Germany). Poly(dimethyl siloxane) (PDMS) and poly(tetrafluoro ethylene) (PTFE, Bess Medizintechnik GmbH, Berlin, Germany) were used as reference surfaces with low and high thrombogenicity, respectively. Material surface adherent platelets were visualized by the glutardialdehyde induced fluorescence technique and quantified microscopically as described previously [17].

RESULTS

Synthesis of thin layer coating and alteration of surface properties

The in situ synthesis of thin hydrogel coatings directly at the material surface involved the immobilization of the biocatalyst HRP at the material surface as a first step. As model surfaces, either amine functionalized glass or gold surfaces with deposition of self-assembled monolayers bearing free primary amines were employed. The coupling of HRP was conducted with the help of glutaraldehyde (Fig. 1). The binding of HRP was, as described later, in most cases conducted at pH 7.1. This roughly matches an average isoelectric point (pI) of HRP, which is based on the relative contribution of the different isoenzymes, and particularly corresponds to the range of pI of isoenzyme C subfractions [18] that are known to be most prevalent in commercial HRP preparations [19] [20] [21]. Additionally, in some parts of this study, potential effects of pH shifts on HRP immobilization were evaluated by exploring pH 6.0 for HRP coupling. At pH 6.0, the protonation state of primary amine groups would be higher and thus less preferred, while stability of the enzyme's active center and secondary structure is still given [22] [23].
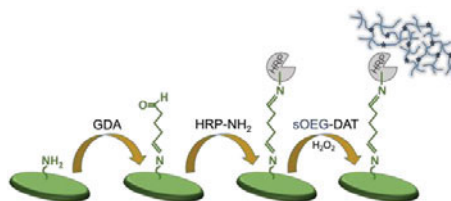
Fig. 1: Scheme of steps for surface functionalization and vision of enzyme-catalyzed thin layer hydrogel coating. The immobilized HRP should convert DAT moieties into corresponding phenoxyl radicals, which are further reacting to form covalent netpoints (stars) connecting several oligoethylene arms. A color version of the figure is available online.

When sOEG-DAT was incubated with HRP treated surfaces, a thin hydrogel layer was expected to be formed. Conceptually, this reaction involves the reductive cleavage of H_2O_2 by HRP in the presence of an electron donor (phenolic hydroxyl moieties of DAT), thus creating phenoxyl radicals. Such radicals can react in radical coupling reactions, with an assumed formation of DAT-derived netpoints between several oligoethylene chains leading to a large and insoluble network material.

In a visual inspection, the formation of a coating could not be detected. However, considering the performed chemical modification, a change in the physicochemical properties of the surfaces can be expected. The analysis of contact angles θ illustrated a systematic trend towards increased wettability with water, i.e. reduced θ (Fig 2A). Both the advancing angle corresponding to wetting and the receding angle mimicking de-wetting were < 65° for hydrogel coated surfaces, a value often considered as functional indicator ("Berg's limit") for surface shielding from undesired protein adsorption [6] [24].

Along with the surface functionalization process, an alteration of surface charges can be expected. Starting from amino-terminated moieties with a determined positive zeta potential of +14 mV, introduction of aldehyde functions resulted in a conversion towards -21 mV with a subsequent decrease to -16 mV upon coupling HRP. The incubation with sOEG-DAT for hydrogel coating was associated with a further decrease of the zeta potential towards the neutral range, in which a value of -1 mV was determined. These data suggest a shielding of the surface through the hydrogel layer formed.
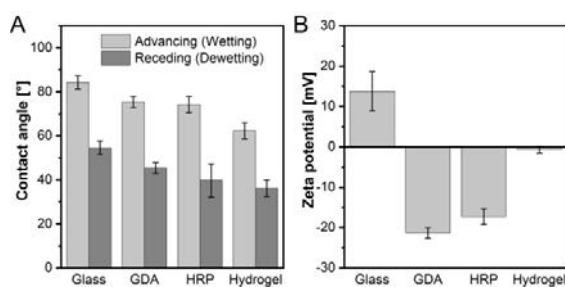
Fig. 2: Physicochemical characterization of surface properties. (A) Contact angle: Each sample was analyzed at a minimum of two positions with a total of ≥10 individual measurements in both advancing and receding mode (mean, SD). (B) Zeta potential: Data of three samples per condition with three measurements each are presented (mean, SD).

Qualitative and quantitative analysis of surface coating

While the physicochemical characterization data reported above strongly suggest successful hydrogel formation, they do not present structural proof that a coating has been deposited, nor do they allow estimation of the kinetics of hydrogel formation or provide information on the thickness of the coating being formed. In order to investigate the chemical composition of the surface, ToF-SIMS has been applied to dried samples. Here, the qualitative determination of $-CH_2CH_2O-$ motifs, the repetitive units of sOEG, is exemplarily depicted as determined either in the positive ($C_2H_5O^+$; m/z 45.04) or the negative ($C_2H_3O^-$; m/z 43.02) ionization mode (Fig. 3). Considering the extensive washing of samples after incubating HRP with its substrate, sOEG-DAT, for enzymatic conversion, the presence of a saturated signal of m/z 45 clearly confirms that sOEG is available in substantial quantities and appears to be permanently bound to the surface (Fig. 3A). This is what would be expected for the HRP catalyzed oxidation and subsequent crosslinking reaction of DAT moieties, leading to the formation of a covalent hydrogel network structure that is swollen and insoluble. When comparing signal intensities from pure sOEG-DAT adsorption to HRP functionalized glasses (without presence of H_2O_2 as the cofactor required for DAT oxidation) to hydrogel synthesis conditions, a much higher amount of sOEG was semi-quantitatively detected in case of enzymatic conversion of sOEG-DAT (Fig. 3A). In a mapping experiment, the distribution of signal intensities of the sOEG repeating unit versus m/z 76.97 corresponding to SiO_3H^- from the underlying glass was characterized for a larger area of the sample surfaces. Signals corresponding to the coating were detected in all portions of the samples, except a number of defects which were dominated by signals corresponding to SiO_3H^- (Fig. 3B). Based on their shape, these defects appear to be scratches arising from sample handling, which may have caused removal of hydrogel layers prior to ToF-SIMS analysis. However, it may also be possible that defects in the initial functionalization with amino groups, which is the basis of all subsequent synthesis steps, have been present in the glass support material or were introduced when cutting them to the desired sizes. It should be noted that Fig 3B does not provide an information of the signal distribution in the z-axis. Furthermore, the ToF-SIMS technique relies on analysing dry samples, thus collapsing of the hydrogel layers occurs during sample preparation with potential drying artefacts. While no large uncoated areas of definite round shape as typical for coating defects were detected, at least in the upper left corner of Fig 3B some signals corresponding to m/z 76.97 are visible in mixture with m/z 43, which may be due to collapse of the dried hydrogel or coating imperfection.
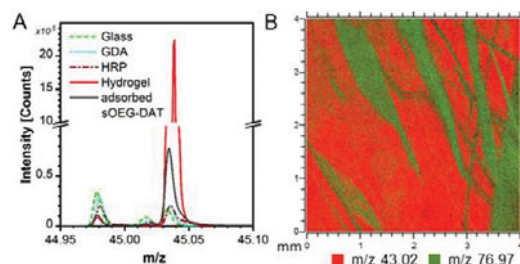
Fig. 3: Chemical analysis of functionalized surfaces by ToF-SIMS. (A) Semi-quantitative determination of ethylene glycol repeat units detected via the fragment $C_2H_5O^+$, 45.04 m/z, at the different stages of functionalization. For comparison, pure sOEG-DAT adsorption to HRP functionalized glasses without presence of cofactor H_2O_2 is presented as a negative control. All measurements were conducted after rinsing the treated surfaces. (B) Mapping of surface composition with oligo(ethylene glycol) coating identified by $C_2H_3O^-$ (m/z 43.02) and underlying glass, SiO_3H^- (m/z 76.97), the latter being present in presumably scratched sample areas. A color version of the figure is available online.

In order to quantitatively monitor the hydrogel formation kinetics and coating thickness depending on different experimental conditions, the QCM technique was applied. The amino-functionalized gold sensors of the QCM were consecutively flushed with the respective reagents until an equilibrium of frequency shifts could be determined (Fig. 4A). As can be seen from the slope of the curve upon sOEG-DAT addition, a thickness of 90% of the final hydrogel coating thickness was obtained within less than 10 minutes. By the Kevin-Voigt model for viscoelastic materials, which is applicable for adsorbed soft materials or hydrogels that do not flow and preserve their shape [25], coating thicknesses could be calculated. While the pure adsorption of sOEG-DAT to gold sensors resulted in thicknesses of 88 ± 1 nm, clearly higher values of roughly 250 nm were determined for HRP-catalyzed hydrogel coating. Interestingly, this process appeared robust, as small pH shifts from pH 7.1 (coating 247 ± 23 nm) to pH 6.0 (coating 249 ± 20 nm) did not affect coating thickness.
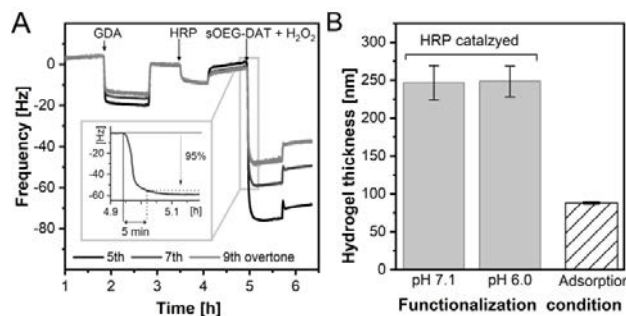

Fig. 4: Quantitative analysis of layer thicknesses by QCM. (A) Experimental steps and exemplary curves of 5th, 7th and 9th overtone. (B) Hydrogel layer thickness depending on synthesis condition as determined by the Kevin-Voigt model (n=3, mean, SD).

As an independent method to assess coating thickness and integrity, AFM was applied. In a mapping experiment with hydrated samples, a homogeneous coating was observed (Fig. 5A). In a scratch test, the depth profiles (z axis) of the sample indicated a coating layer thickness of 115 ± 51 nm on glass surfaces (Fig. 5B). While both methods, AFM and QCM, display coating thickness in the medium nanometer size range, the slight differences in values might be assigned to the respective principles and conditions of the method or the different surfaces being used (glass/gold), possibly leading to different contents or activities of bound HRP.
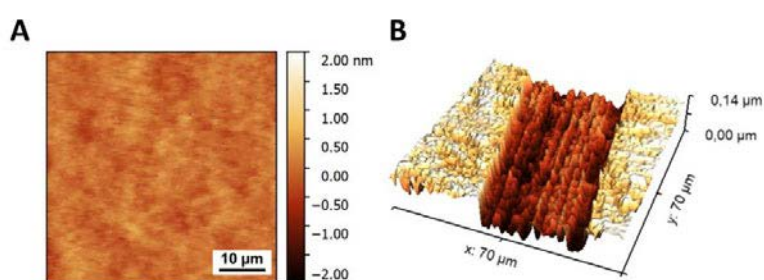

Fig. 5: Characterization of sample surfaces by AFM in aqueous environment. (A) Homogeneous topography of sample surface. (B) Micrograph of a scratch on sample surface used for determination of coating layer thickness.

Functional evaluation of surface coating

Thin hydrogel coatings offer potential for a variety of application fields, ranging from, e.g., coatings on cell culture systems, protein/biofilm repellence in technical applications, or sensors based on flexible electronics. Here the interaction with human blood platelets has exemplarily been selected for functional evaluation of the coating in view of potential full blood bioanalytics. Testing under quasi-static conditions allowed an estimation of the thrombogenic potential of the coatings, based on the number of adherent platelets as well as their activation state. When material-surface adherent platelets become activated, they undergo a morphological transition from a discoid to a spread-out shape. In this study, surfaces with HRP-catalyzed sOEG-DAT hydrogel coatings showed lower densities of adherent platelets ($1.0 \times 10^3 \pm 0.9 \times 10^3$ platelets per mm^2) than the thrombogenic control, PTFE ($6.6 \times 10^3 \pm 3.2 \times 10^3$ platelets per mm^2), as well as untreated glass ($2.3 \times 10^3 \pm 0.9 \times 10^3$ platelets per mm^2) (Fig. 6A). Furthermore, there was no significant difference in platelet density compared to PDMS ($0.5 \times 10^3 \pm 0.5 \times 10^3$ platelets per mm^2), a low thrombogenic material that is generally accepted for its hemocompatibility, employed in bioanalytical devices for whole blood analysis [26], and even used in surgical implants. The microscopic investigation of platelet shape clearly showed that the few adherent platelets were in a non-activated state, while more spread platelets were detected on non-modified glass and PTFE (Fig. 6B). The observed background contrast for PDMS and sOEG-DAT hydrogel coated glass samples has been interpreted as an interaction of the coating with the fluorescent fixative glutardialdehyde. Overall, the hydrogel coating showed a low thrombogenicity suggesting its suitability for blood contacting surfaces in bioanalytics as a potential application.
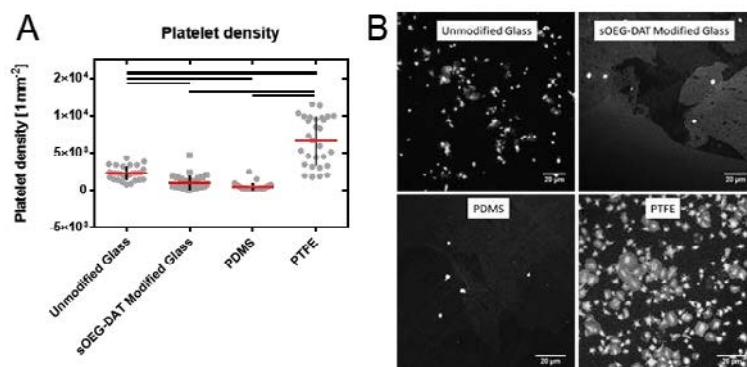
Fig.6: *In vitro* analysis of the thrombogenicity in a quasi-static test setup for unmodified glass, sOEG-DAT modified glass, poly(dimethyl siloxane) (PDMS; negative control), and poly(tetrafluoro ethylene) (PTFE; positive control). (A) Quantitative data of the density of adherent platelets. Gray dots: data points; Horizontal lines: arithmetic mean; Crossing lines: S.D.; n=3 donors with 2 material repeats per donor; Statistical analysis by Kruskal-Wallis Test with Dunn's multiple comparison test: bars represent $p<0.05$). (B) Representative images of adherent platelets from healthy subjects by confocal laser scanning microscopy (Scale bar=20 μm, 100 fold primary magnification).

Discussion

The analytical data collected for HRP catalyzed deposition of sOEG-DAT based hydrogels at model surfaces suggest that the concept can be realized in principle. It should be noted that the process involves several steps, each of them critically contributing to successful hydrogel synthesis. At the same time, each step may not be quantitative, e.g., the GDA reaction with amine moieties of the glass support and subsequent enzyme coupling are typically not consuming all of the available reactive moieties of the previous step, thus resulting in their continuous presence during hydrogel synthesis. Besides those amine and aldehyde moieties, also the network precursor, sOEG-DAT, contributes free primary amino groups from non-functionalized arms. Further functional groups are present from amino acid side chains of HRP and its protoporphyrin-based active center. In this complex setting, phenoxyl radicals formed in the catalytic cycle of HRP may react with themselves and not yet activated phenols of DAT moieties, but potentially also undergo side reactions with other available moieties. In fact, the stepwise inactivation of HRP by phenoxyl radicals has been assigned to a combination of different mechanisms, including chemical coupling to protoporphyrin [27]. While the rate constants of phenoxyl radical reactions with themselves are typically a few orders of magnitude higher than the reaction e.g. with amines or thiols [28], theoretically also cascade reactions with free amine groups such as from the support surface or the sOEG might be possible as side reactions. Such pathways would add additional complexity to the formed structures, but may not impede their ability to act as a hydrogel shielding of the surface.

Other than small molecule substrates of HRP, DAT is coupled to sOEG as polymer network precursor, which restricts its mobility/diffusivity. Accordingly,

hydrogel formation originates from a multitude of local foci around the immobilized enzyme molecules and spatially proceeds within the range of phenoxyl radial diffusion. The hydrogel formation will be stopped when no further sOEG-DAT can diffuse to the active center through the already formed hydrogel layer, which was detected to be ~115 nm or ~250 nm depending on the analytical technique. Also, HRP inactivation might be involved [27]. Eventually, the enzyme will be entrapped within the hydrogel, which is inhomogeneous on the molecular level.

In contrast to surface modification by direct coupling of hydrophilic polymer chains to surfaces, e.g. as self-assembled monolayers, a direct chemical bonding between hydrogel and surface is not inherent to the concept. However, no detachment of the hydrogel coatings from the support was observed, suggesting either physical interaction or chemical bonding through side reactions as introduced above. Entanglement of surface-immobilized HRPO within the formed hydrogel network may contribute to coating fixation to the support.

Despite applied to flat model surfaces, the approach presented here should be applicable also to three dimensional objects of various shapes where enzymes can be immobilized. In this respect, the concept differs, e.g., from spin-coating-based approaches, which would be able to provide similar or larger coating thicknesses, and compares, e.g., to polydopamine or layer-by-layer coating strategies. The thickness of polydopamine coatings is scalable in chemical vapour deposition techniques [29] but remains below 50-100 nm and proceeds to such maximum values with very slow kinetics in solution based processes [30], thus staying – in a comparable technique – below the dimensions of coatings obtained here by HRP.

A wide range of applications may be envisioned for this coating concept in biotechnology, medicine and various technical fields. However, based on the radical reaction during hydrogel crosslinking, it may not be possible to entrap molecules such as pharmaceutics in the hydrogel as they might undergo chemical alteration during network formation. For potential use as coatings of implant materials, a risk analysis may need to consider potential immunogenic reaction to plant derived HRP entrapped in the hydrogel. However, in the medical field, bioanalytical applications including point-of-care diagnostic devices could make us of this coating technology.

CONCLUSIONS

In this study, the suitability of enzymatic catalysis to build hydrogel layers from sOEG-DAT at surfaces could be demonstrated. The characterization of surface properties demonstrated a hydrophilic shielding of the model matrix material, while QCM, AFM and ToF-SIMS proved successful deposition of hydrogels with thicknesses in the ~250 nm size range, while adsorption without HRP catalysis resulted in much thinner (~90 nm) layers. In a demonstrator experiment, a hemocompatibility similar to non-thrombogenic reference materials was observed. Overall, the successful "coating-from" approach may in the future be applied to various shapes of surfaces, e.g. for coatings of cell culture systems, protein/biofilm repellence in technical applications, or in flexible electronics.

ACKNOWLEDGMENTS

REFERENCES

1. M. E. Nash, W. M. Carroll, P. J. Foley, G. Maguire, C. O. Connell, A. V. Gorelov, S. Beloshapkin and Y. A. Rochev, *Soft Matter* **8** (14), 3889-3899 (2012).
2. S. Y. Zheng, Y. Tian, X. N. Zhang, M. Du, Y. Song, Z. L. Wu and Q. Zheng, *Soft Matter* **14** (28), 5888-5897 (2018).
3. D. Moreau, C. Chauvet, F. Etienne, F. P. Rannou and L. Corte, *Proc. Natl. Acad. Sci. USA* **113** (47), 13295-13300 (2016).
4. A. Mateescu, Y. Wang, J. Dostalek and U. Jonas, *Membranes (Basel)* **2** (1), 40-69 (2012).
5. W. Cheng, X. W. Zeng, H. Z. Chen, Z. M. Li, W. F. Zeng, L. Mei and Y. L. Zhao, *ACS Nano* **13** (8), 8537-8565 (2019).
6. Q. Wei, T. Becerer, S. Angioletti-Uberti, J. Dzubiella, C. Wischke, A. T. Neffe, A. Lendlein, M. Ballauff and R. Haag, *Angew. Chem. Int. Edit.* **53** (31), 8004-8031 (2014).
7. Q. M. Dudley, A. S. Karim and M. C. Jewett, *Biotechnol. J.* **10** (1), 69-82 (2015).
8. S. Z. Ren, C. H. Li, X. B. Jiao, S. R. Jia, Y. J. Jiang, M. Bilal and J. D. Cui, *Chem. Eng. J.* **373**, 1254-1278 (2019).
9. X. Wang, S. S. Chen, D. B. Wu, Q. Wu, Q. C. Wei, B. He, Q. H. Lu and Q. G. Wang, *Adv. Mater.* **30** (17), 1705668 (2018).
10. M. Bilal and H. M. N. Iqbal, *Catal. Lett.* **149** (8), 2204-2217 (2019).
11. C. Wischke, E. Bahr, M. Racheva, M. Heuchel, T. Weigel and A. Lendlein, *MRS Adv.* **3** (63), 3875-3881 (2018).
12. S. Sakai and M. Nakahata, *Chem.-Asian J.* **12** (24), 3098-3109 (2017).
13. M. Khanmohammadi, M. B. Dastjerdi, A. Ai, A. Ahmadi, A. Godarzi, A. Rahimi and J. Ai, *Biomater. Sci.* **6** (6), 1286-1298 (2018).
14. B. O. Burek, S. Bormann, F. Hollmann, J. Z. Bloh and D. Holtmann, *Green Chem.* **21** (12), 3232-3249 (2019).
15. K. K. Julich-Gruner, T. Roch, N. Ma, A. T. Neffe and A. Lendlein, *Clin. Hemorheol. Microcirc.* **60** (1), 13-23 (2015).
16. S. Braune, C. Sperling, M. F. Maitz, U. Steinseifer, J. Clauser, B. Hiebl, S. Krajewski, H. P. Wendel and F. Jung, *Colloid Surface B* **158**, 416-422 (2017).
17. S. Braune, G. Alagoz, B. Seifert, A. Lendlein and F. Jung, *Clin. Hemorheol. Microcirc.* **52** (2-4), 349-355 (2012).
18. F. W. Krainer and A. Glieder, *Appl. Microbiol. Biot.* **99** (4), 1611-1625 (2015).
19. N. C. Veitch, *Phytochemistry* **65** (3), 249-259 (2004).
20. J. N. RodriguezLopez, J. HernandezRuiz, F. GarciaCanovas, R. N. F. Thorneley, M. Acosta and M. B. Arnao, *J. Biol. Chem.* **272** (9), 5469-5476 (1997).
21. M. C. Hoyle, *Plant Physiol.* **60** (5), 787-793 (1977).
22. K. Chattopadhyay and S. Mazumdar, *Biochemistry* **39** (1), 263-270 (2000).
23. M. A. Lemos, J. C. Oliveira and J. A. Saraiva, *Lebensm.-Wiss. Technol.* **33** (5), 362-368 (2000).
24. E. A. Vogler, *Adv. Colloid Interfac.* **74**, 69-117 (1998).
25. T. P. McNamara and C. F. Blanford, *Analyst* **141** (10), 2911-2919 (2016).
26. J. H. Son, S. H. Lee, S. Hong, S. M. Park, J. Lee, A. M. Dickey and L. P. Lee, *Lab Chip* **14** (13), 2287-2292 (2014).
27. Q. Huang, Q. G. Huang, R. A. Pinto, K. Griebenow, R. Schweitzer-Stenner and W. J. Weber, *J. Am. Chem. Soc.* **127** (5), 1431-1437 (2005).
28. P. Neta and J. Grodkowski, *J. Phys. Chem. Ref. Data* **34** (1), 109-199 (2005).
29. H. Coskun, A. Aljabour, L. Uiberlacker, M. Strobel, S. Hild, C. Cobet, D. Farka, P. Stadler and N. S. Sariciftci, *Thin Solid Films* **645**, 320-325 (2018).
30. V. Ball, D. Del Frari, V. Toniazzo and D. Ruch, *J. Colloid Interf. Sci.* **386**, 366-372 (2012).